Asian Journal of Chemistry; Vol. 35, No. 6 (2023), 1509-1517

ASIAN JOURNAL OF CHEMISTRY

https://doi.org/10.14233/ajchem.2023.27808

Synthesis, Spectral Investigation, DFT, Antibacterial, Antifungal and Molecular Docking Studies of Ni(II), Zn(II), Cd(II) Complexes of Tetradentate Schiff-Base Ligand

T. MURUGAN[1], RANGASWAMY VENKATESH[1,*], KANNAPPAN GEETHA[1] and ALY ABDOU[2]

[1]P.G. & Research Department of Chemistry, Muthurangam Government Arts College (Autonomous), Vellore-632002, India
[2]Department of Chemistry, Faculty of Science, Sohag University, Sohag-82534, Egypt

*Corresponding author: E-mail: venkatmoksharakshan@gmail.com

Received: 31 March 2023; *Accepted*: 9 May 2023; *Published online*: 27 May 2023; AJC-21270

By refluxing 4-nitro-*o*-phenylenediamine and 5-nitro salicylaldehyde, a new Schiff base ligand was synthesized. By reacting the appropriate precursor with the tetradentate Schiff base ligand, three nitro-substituted nickel(II), zinc(II) and cadmium(II) complexes were synthesized. UV-Visible, FTIR and ^{1}H NMR spectral investigations were used to characterize the ligand. Molar conductance, LC-MS, UV-visible and FTIR spectrum analysis were used to characterize the synthesized metal(II) complexes. The ligand and metal(II) complexes were also tested for antibacterial activity. DFT simulations were performed at the B3LYP/6-311G (d,p) and LanL2dz levels of theory were utilized to study the geometry of the Schiff base ligand and the metal(II) complexes. In addition, the molecular orbital occupancy of HOMO and LUMO, as well as the molecular electrostatic potential (MEP), were computed. Molecular docking investigation were conducted utilizing the active sites of the *E. coli* FabH-CoA complex (PDB ID: 1HNJ) receptor in order to detect the interactions between metal(II) complexes and define their likely binding locations.

Keywords: Metal(II) complexes, Tetradentate Schiff base ligand, Antimicrobial activity, DFT studies, Molecular docking.

INTRODUCTION

Considering the numerous uses for Schiff bases and their metal complexes, coordination chemistry has advanced and there is still much difficult work to be done on Schiff base metal(II) complexes and their many industrial applications [1]. A geometric restriction is frequently imposed by the system in a Schiff base and this has an impact on the electrical structure as well [2,3]. The C=N linkage is essential necessary for biological action in azomethine derivatives. There have been numerous reports of azomethines having exceptional antibacterial and antifungal properties [4-7]. Schiff bases are used in a variety of industrial, analytical, catalytic, agrochemical and biological processes [8]. They have attracted a lot of attention from the scientific community because they are easy to synthesize and complexation with the metals. Regarding the evaluation of novel, more effective antibacterial medicines with little toxicity, due to their structural collection and preparative accessibility, Schiff base complexes are found to be the most significant stereochemical models in main group and transition metal coordination chemistry [9].

To better understand the structure and biological activities of biomolecules, Schiff base transition metal complexes have been used as biological models. Thus, in this work, we describe the synthesis of symmetric tetradentate Schiff base derived from 4-nitro-*o*-phenylenediamine and 5-nitrosalicylaldehyde and its metal complexes of nickel, zinc and cadmium and their biological characteristics.

EXPERIMENTAL

All chemicals and solvents procured in this work were used without further purification. 5-Nitrosalicylaldehyde and 4-nitro-*o*-phenylenediamine was purchased from Sigma-Aldrich, USA, whereas the metal(II) acetate were procured from Spectrochem Pvt. Ltd. The infrared spectra were recorded using KBr discs in the 4000-400 cm^{-1} range. The ^{1}H NMR spectrum was recorded in DMF and the chemical shifts were compared to tetramethylsilane (TMS) as an internal standard.The UV-visible spectrophotometer was used to record the spectrum at room temperature. The DMF as the solvent was used to analyzed the conductivity measurements.

Synthesis of Schiff base ligand (L_1): A solution of 5-nitrosalicylaldehyde (20 mmol) dissolved in 20 mL of ethanol was added to an ethanolic solution of 4-nitro-*o*-phenylenediamine (10 mmol) and stirred for 30 min using magnetic stirr followed by 6 h of refluxation at 80 ºC and then finally cool to room temperature. After some time, a yellow solid precipitate was filtered, washed with warm ethanol and dried (**Scheme-I**).

Synthesis of metal(II) complexes: A Schiff base ligand solution (2 mmol) in 20 mL in absolute ethanol was added to a ethanolic solution of corresponding metal(II) acetate (2 mmol) and stirred for 30 min using magnetic stirr followed by 6 h of refluxation at 80 ºC and then finally cool to room temperature. The filtered precipitate washed with distilled water then dried after being rinsed with hot ethanol (**Scheme-I**).

DFT calculations: The programs GAUSSIAN 09 [10,11] and CHEMBIODRAW Ultra 12.0 [12,13] were utilized throughout all of the computational procedures involving the synthesized Schiff base ligand as well as its metal(II) complexes. Using the density functional theory (DFT), with Becke 3-parameter (exchange) Lee-Yang-Parr (B3LYP) [14,15] with the LANL2DZ basis set [16,17] for the metal atoms and the 6-311G(d,p) basis set [18,19] established for the other atoms, the geometries of the examined metal(II) complexes were entirely optimized. Some quantum chemical parameters, such as ionization potential (IP), electron affinity (EA), energy gap (ΔE), electronegativity (χ), chemical potential (μ), chemical hardness (η), softness (σ) and electrophilicity index (ω), nucleophilicity index (Nu) and maximum electronic charge (ΔN_{max}) were determined by using HOMO and LUMO energies [20-24].

Molecular docking investigation: In order to validate the therapeutic potential of the compounds in question, a molecular docking analysis was run on them against the 1HNJ protein utilizing the MOE package. The 1HNJ code refers to the FabH-CoA complex in *E. coli*. The FabH receptor is thought to be the target when attempting to determine the antibacterial capabilities of compounds found in nature [25]. FabH has a role in the production of fatty acids through the process of biosynthesis. From the protein database (http://www.rcsb.org), we were able to get the three-dimensional structure of the target protein receptor. The substances that were being examined served as the substrate. An examination of molecular docking was carried out with the use of the molecular overeating environment (MOE) program. In order to prepare the substrate, each chemical was first optimized using the process of energy minimization, then a new database was created and the file was eventually stored in MDB format. In order to prepare the receptor, the target receptor was subjected to the addition of hydrogen atoms, the connection of different types of receptors, the fixing of potential energy and lastly, the search for active pockets and the production of dummies. To assess the nature of the interactions and rate the inhibitory activity according to the scoring function (S, kcal/mol), docking patterns and interaction parameters were exported [26].

RESULTS AND DISCUSSION

The multiplet signal between δ 7.8 and 8.4 ppm in the ^{1}H NMR spectrum of the synthesized Schiff base ligand can be attributed to the azomethine group (-HC=N). The aromatic protons were responsible for the multiplet signal observed at δ 6.90 ppm.

Conductance studies: The low molar conductance values of the synthesized metal(II) complexes lies in the range of 5 to 7.2 (ohm^{-1} cm^2 mol^{-1}) shows that all the metal(II) complexes behave like non-electrolytes [27,28]. The values of the molar conductance of the metal(II) complexes and Schiff base ligands are provided in Table-1.

UV-visible studies: The UV-visible spectral data of the Schiff base ligand and its metal(II) complexes are shown in Table-1. The π-π* benzene transition of Schiff base ligand is responsible for the 279 nm band. A band at 349 nm is attributed to the π-π* transition of the azomethine group (-HC=N)- in the ligand. The band at 490 nm was also appeared because of

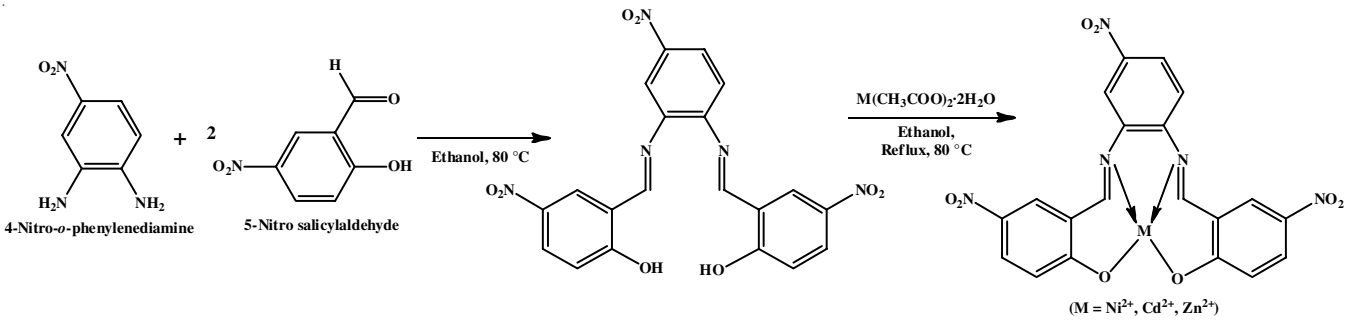

Scheme-I: Synthesis of Schiff base ligand and its metal(II) complexes

TABLE-1
MOLAR CONDUCTANCE AND UV-VISIBLE SPECTRAL DATA OF SCHIFF BASE LIGAND AND ITS METAL(II) COMPLEXES

Compound	m.f.	m.w.	Molar conductance (ohm^{-1} cm^2 mol^{-1})	UV-visible spectral data			
				π–π* (nm) (benzene)	π–π* (nm) (-HC=N)	n–π*(nm)	*d-d* (nm)
Schiff base ligand	$C_{20}H_{13}N_3O_8$	451.34	–	279	349	490	–
Ni^{2+} complex	$C_{20}H_{11}N_5O_8Ni$	508.02	7.1	271	348	491	546
Zn^{2+} complex	$C_{20}H_{11}N_5O_8Zn$	514.71	5.0	277	346	491	–
Cd^{2+} complex	$C_{20}H_{11}N_5O_8Cd$	561.74	7.2	278	348	483	–

the n-π* transition of Schiff base ligand. The presence of benzene ring in the metal(II) complexes led to the observation of an experimental band in the range of 271-278 nm, whereas the azomethine group (-HC=N) in the complexes exhibited a π-π* transition, resulting in the appearance of band at 346-348 nm. The n-π* transition of the complexes is responsible for the band at 483-491 nm. A new band at 546 nm was due to *d-d* transition of the complex. The UV-visible spectrum of all the metal(II) complexes are shown in Fig. 1.

FT-IR studies: The key FT-IR spectral data of the synthesized metal complexes and ligand are given in Table-2. A peak at 1616 cm^{-1} is due to the stretching frequency of the azomethine group (-HC=N) in the ligand. The peak at 1335 cm^{-1} is assigned to C-O stretching vibration of the ligand, whereas the peak at 3375 cm^{-1} has been attributed to the ligand -OH stretching vibration. The azomethine group of the ligand caused the peak at 1616 cm^{-1}, which shifted to a lower frequency after the metal(II) complexation (1613-1605 cm^{-1}) and thus confirmed the metal coordination with azomethine nitrogen. The peak at 1334-1306 cm^{-1} region was due to C-O stretching vibrations of the complexes. The peak at 3365-3083 cm^{-1} was due to complexes coordinated with water molecules [4,28]. The peak at 480-406 cm^{-1} was due to ν(M-O(stretching vibrations of the complexes, wheras the peak at 517-474 cm^{-1} was observed due to ν(M-N) stretching vibration of the complexes.

TABLE-2
FT-IR SPECTRAL DATA OF THE LIGAND AND THE METAL(II) COMPLEXES

Compound	ν(-C=N)	ν(-C-O)	ν(–OH)	ν(M-O)	ν(M-N)
Schiff base ligand	1616	1335	3375	–	–
Ni^{2+} complex	1605	1309	3083	480	517
Zn^{2+} complex	1613	1334	3108	417	505
Cd^{2+} complex	1606	1306	3365	406	474

Mass spectra: The *m/z* peak in the mass spectra of the Ni^{2+} complex was appeared at 508.18, which agrees well with the calculated molecular weight of 508.02. The mass spectra confirms the formation of the Ni^{2+} complex.

DFT calculations

Optimized complex structures: The Schiff base ligand and its metal(II) complexes with NiL, ZnL and CdL were all

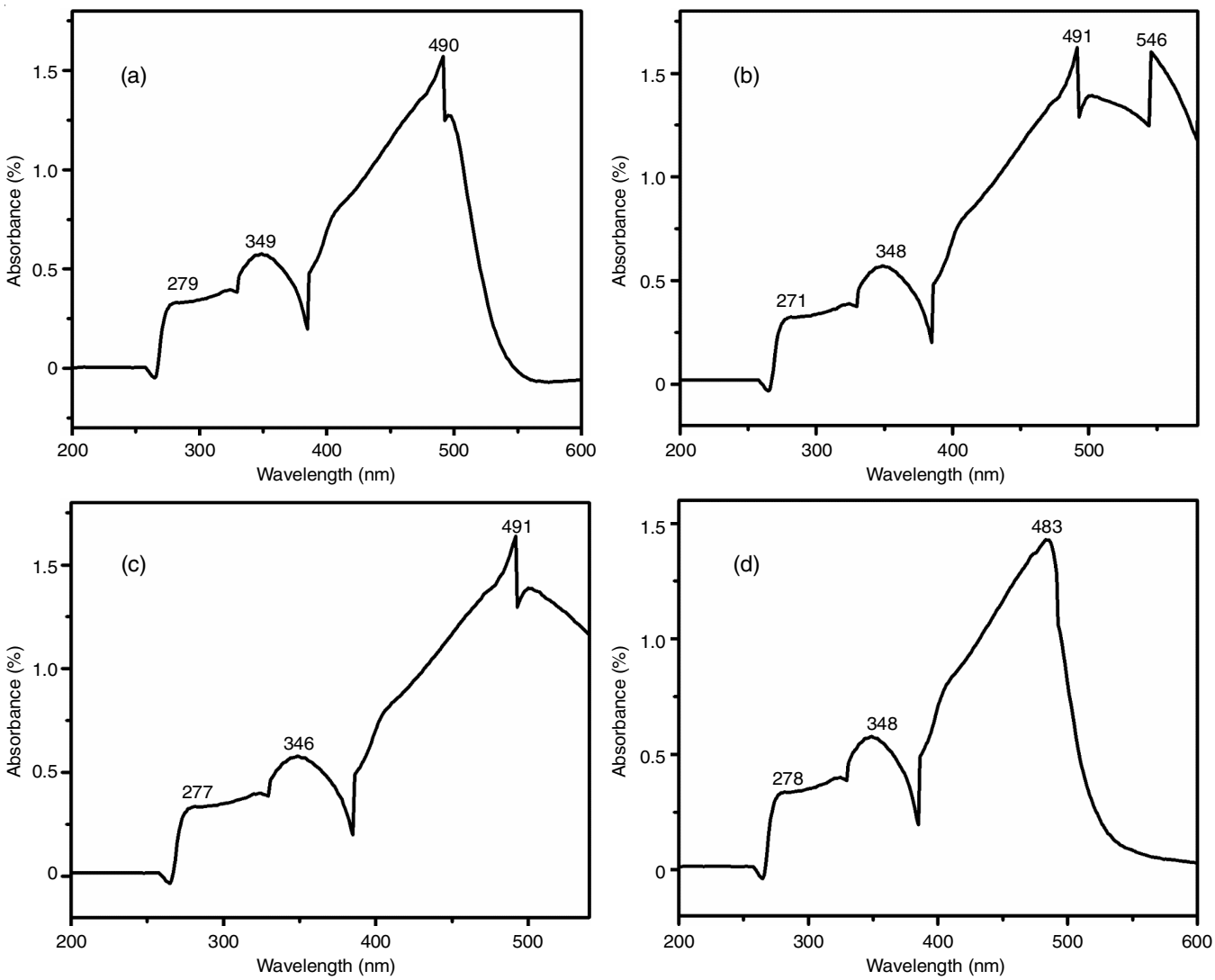

Fig. 1. UV-visible spectrum of the studied compounds (a) Schiff base ligand, (b) Ni^{2+} complex, (c) Zn^{2+} complex and (d) Cd^{2+} complex

subjected to optimizations using the B3LYP method. Fig. 2 presents the optimized three-dimensional structures of Schiff base ligand and its metal(II) complexes. Table-3 presents several estimated structural characteristics, including bond length and bond angle, for the complexes that were investigated.

Through the two phenolic oxygen binding sites and the two azomethine nitrogen binding sites, the metal ion [Ni(II), Zn(II) and Cd(II)] forms a covalent bond with the Schiff base ligand moiety, which results in the formation of a metal complex with four coordinated sites (Fig. 2). Taking into account the bond angles, it is clear that Ni(II) complex and the other metal(II) complexes (Zn^{2+} and Cd^{2+}) exhibited a square planar geometry and a tetrahedral geometry, respectively. To provide additional evidence, the degree of distortion in four coordinate geometry was computed as $\tau_4 = (360-(\alpha+\beta))/141$ [2], where α and β are the two angles that make up the greatest portion of the figure.

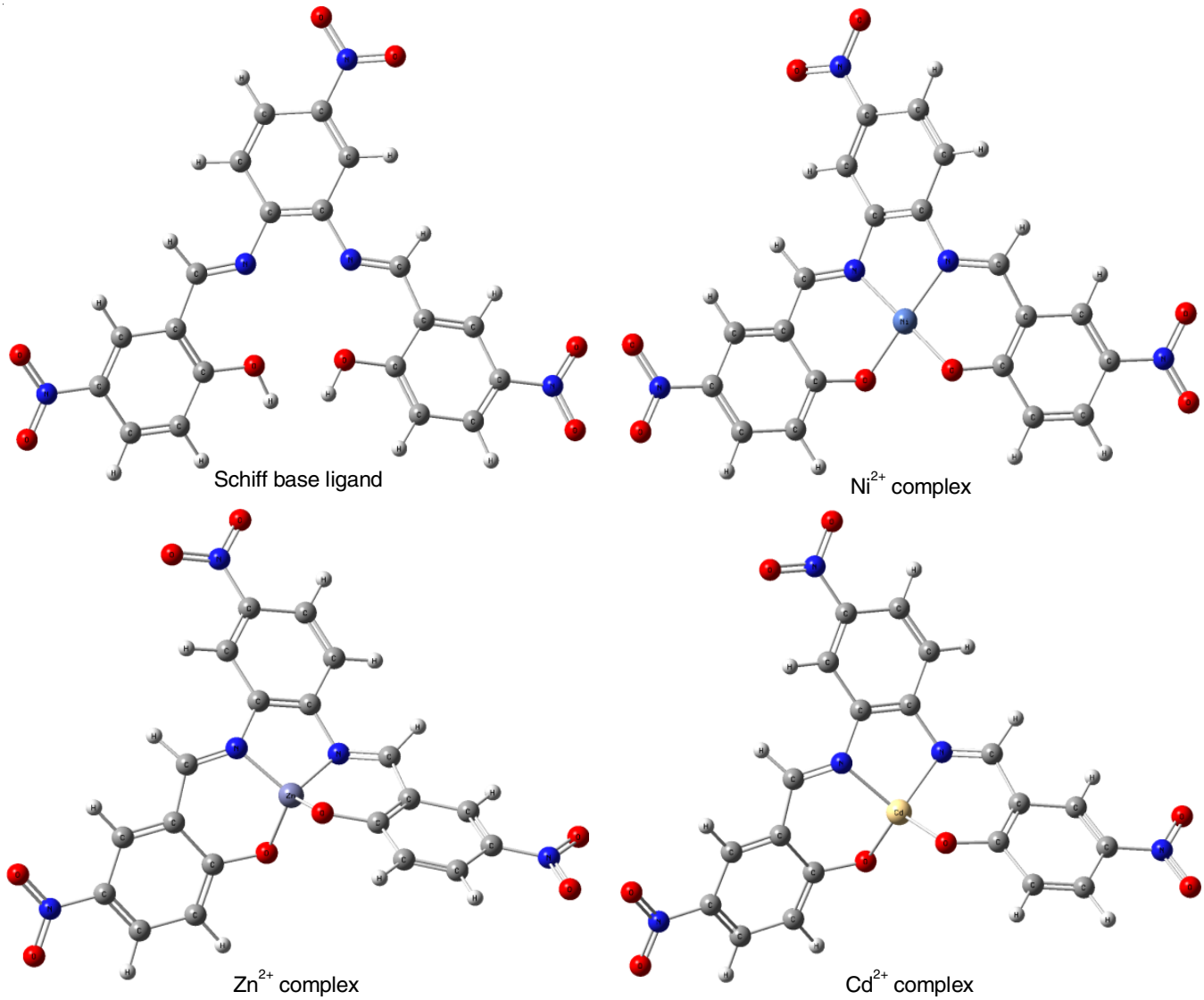

Fig. 2. Optimized structures of the H_2L ligand and its complexes using the DFT/B3LYP approach

TABLE-3
CALCULATED STRUCTURAL PARAMETERS OF THE SCHIFF BASE METAL(II) COMPLEXES BY THE DFT/B3LYP APPROACH

Bond length (Å)				Bond angle (°)					
Ni^{2+} complex									
Ni-O	1.816	Ni-N	1.853	N-Ni-O	88.835	N-Ni-N	84.644	O-Ni-N	171.312
Ni-O	1.814	Ni-N	1.862	N-Ni-O	170.647	O-Ni-O	85.270	O-Ni-N	88.221
Zn^{2+} complex									
Zn-O	1.813	Zn-N	1.809	N-Zn-O	108.982	N-Zn-N	103.365	O-Zn-N	108.982
Zn-O	1.810	Zn-N	1.800	N-Zn-O	118.966	O-Zn-O	115.622	O-Zn-N	116.911
Cd^{2+} complex									
Cd-O	1.813	Cd-N	1.809	N-Cd-O	108.449	N-Cd-N	102.860	O-Cd-N	108.449
Cd-O	1.810	Cd-N	1.800	N-Cd-O	117.390	O-Cd-O	115.057	O-Cd-N	116.339

This degree of distortion, $\tau_4 = 1$ and 0 in tetrahedral and square planar geometry, respectively. The NiL, ZnL and CdL complexes all had the values of 0.13, 0.88 and 0.89, respectively, which linked to a square planar (for NiL) and tetrahedral geometry (for ZnL and CdL).

Frontier molecular orbital (FMO) analysis: Fig. 3 displays the HOMO and LUMO energies, as well as contour diagrams for the FMOs of the complexes being discussed. On the contour diagrams, the various levels of electron density are represented by a variety of hues, specifically red, yellow, green, light blue

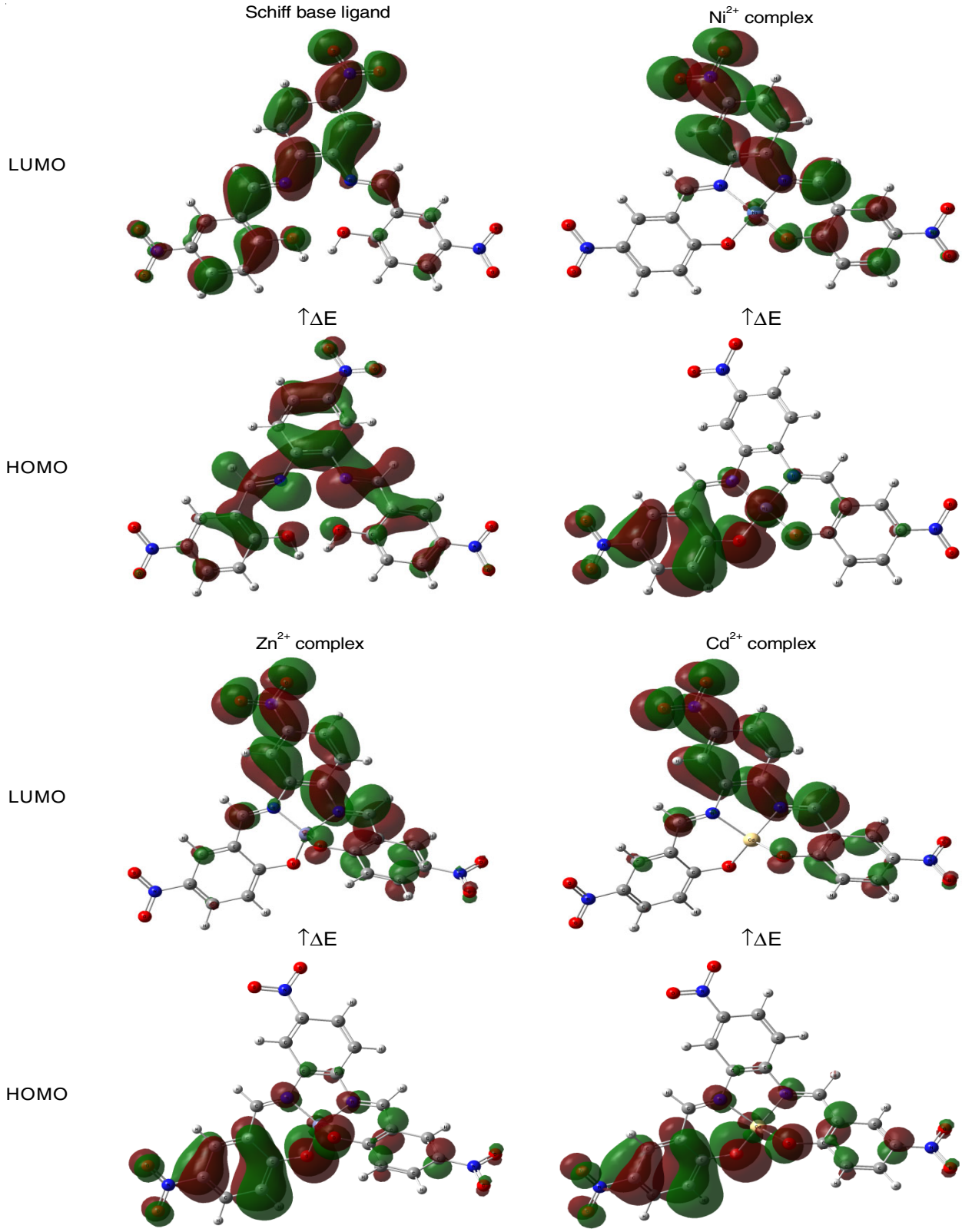

Fig. 3. Contour diagrams of FMOs of the titled compounds

and blue respectively. In the contour diagrams, the regions that correspond to the highest electron density are coloured red and yellow, while the region that corresponds to the lowest electron density is coloured blue. According to Fig. 3, the majority of the electrons that make up the HOMO of the studied complexes are found on the portion of the ligand. The electrons will be focused on the *o*-diamine moiety of the ligand in the complexes if the LUMO is able to accept electrons from the relevant molecule.

Using HOMO and LUMO energies, the quantum chemical parameters, such as ionization potential (IP), electron affinity (EA), energy gap (ΔE), electronegativity (χ), chemical potential (μ), chemical hardness (η), softness (σ) and electrophilicity index (ω), nucleophilicity index (Nu) and maximum electronic charge (ΔN_{max}) were determined. It was found that ZnL and NiL had a smaller energy gap (ΔEg) and η than the cadmium complex. Therefore, ZnL and NiL are softer molecules with higher reactivity and lower kinetic stability. Moreover, ZnL and NiL also have more electrophilicity index than Cd complex with a higher tendency of accepting electrons (Table-4).

Molecular electrostatic potential (MEP): Molecular electrostatic potentials (MEPs) have been used to analyze and forecast the reactive behaviour of a wide range of chemical systems for both electrophilic and nucleophilic processes [29, 30]. Utilizing MEP maps will help to achieve the objective of the stability and relative reactivity of complexes in relation to nucleophiles and electrophiles. Fig. 4 displays various maps of these complexes. The portions of the surface of the molecule shown by the colour red are those in which electron removal may take place most readily (and with the least amount of energy). In addition to this, the red hues signify parts of the surface that have a negative charge (*i.e.* those areas where accepting an electrophile is most favourable). When a complex has a reaction with an electrophile, the relevant sites of the complex will get a negative charge, which symbolizes their attraction to the electrophile. Nitrogen and oxygen atoms have the largest concen-

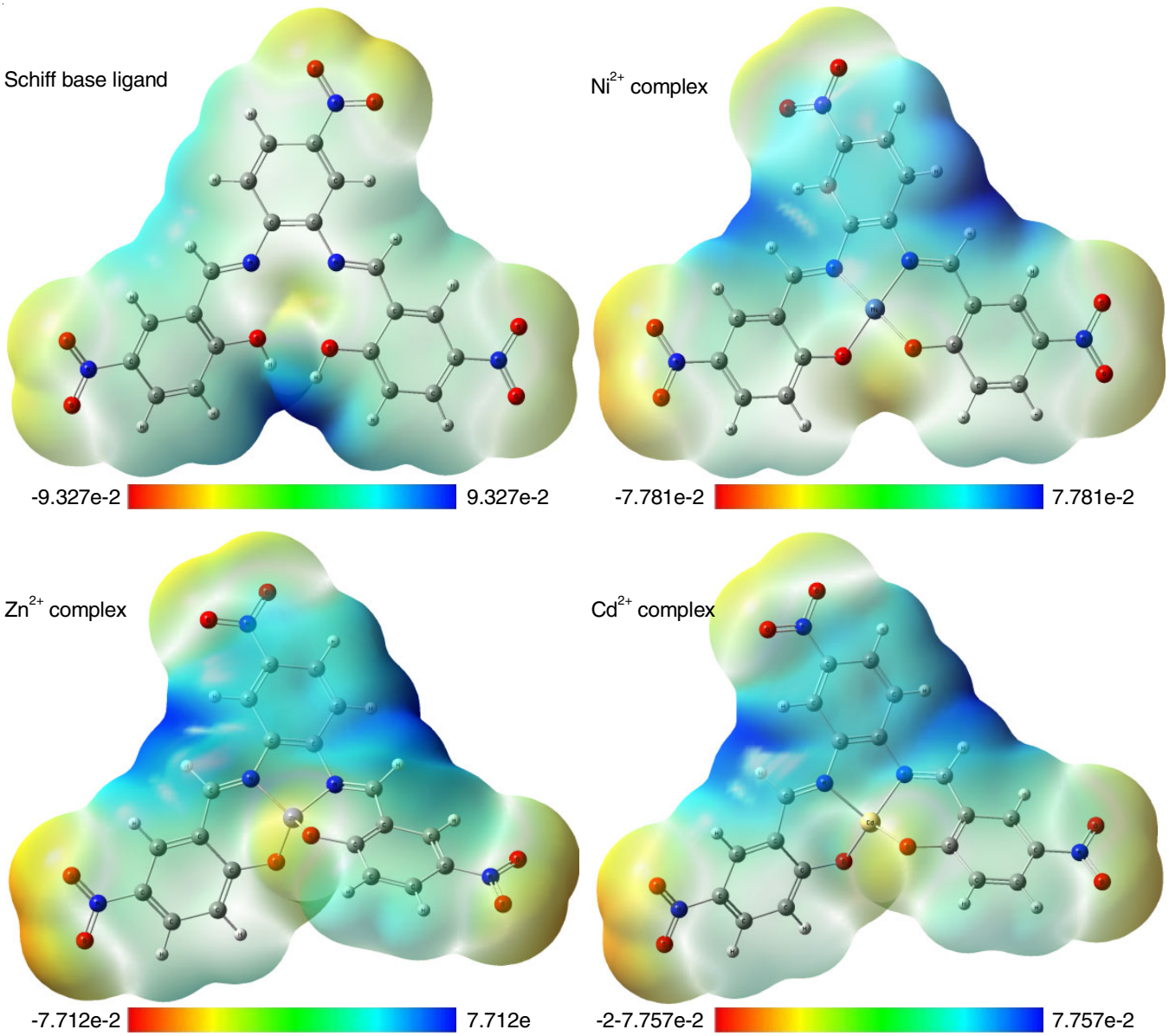

Fig. 4. Molecular electrostatic potential (MEP)

TABLE-4
CALCULATED QUANTUM PARAMETERS OF THE SCHIFF BASE AND ITS METAL(II) COMPLEXES

Compd.	E_{HOMO}	E_{LUMO}	ΔE	I	A	χ	μ	η	S	ω	Nu
Schiff base ligand	-6.72	-3.34	3.38	6.72	3.34	5.03	-5.03	1.69	0.30	7.49	0.133435
Ni^{2+} complex	-6.84	-4.20	2.63	6.84	4.20	5.52	-5.52	1.32	0.38	11.57	0.086416
Zn^{2+} complex	-6.60	-4.24	2.36	6.60	4.24	5.42	-5.42	1.18	0.42	12.44	0.080412
Cd^{2+} complex	-7.07	-4.27	2.80	7.07	4.27	5.67	-5.67	1.40	0.36	11.48	0.087097

trations of negative charges inside the molecule. This provides evidence that these atoms are capable of participating in an electrophilic process. On the other hand, the regions with blue hue signify areas on the molecular surface where electron accepting happens most quickly (with the least amount of energy) and these regions are denoted by the colour blue. In addition, the parts of the surface that are coloured blue signify positively charged regions (*i.e.* those areas where accepting an nucleophile is most favourable). The hydrogen atoms host the largest positive charges, which are concentrated in this region. This provides evidence that these atoms are capable of participating in a nucleophilic process.

Biological activity

Antibacterial activity: The tetradentate Schiff base ligand and its metal complexes were studied for their *in vitro* antibacterial activity against *Escherichia coli*, *Klebsiella pneumonia* (Gram-positive) *Bacillus subtilis* and *Staphylococcus aureus* (Gram-negative) bacterial strains by agar diffusion method. A solution consisting of ligand and metal(II) complexes was distributed over agar plates that had been seeded with different types of bacteria in this method. Incubation was place at 35 ºC for a duration of 27 h using the agar plates. The antibiotic chloramphenicol was used as a standard drug against bacterial strains. The Schiff base ligand and its metal(II) complexes were found to good inhibition all the selected antibacterial microorganisms (Table-5). These findings demonstrated that the metal(II) complexes had significant activity when compared to the Schiff base ligand at different concentrations.

TABLE-5
ZONE OF INHIBITION (mm) OF LIGAND AND ITS METAL(II) COMPLEXES AT VARIOUS CONCENTRATIONS

Strain	Compd.	Control	Concentration (μg/mL)			
			30	60	90	120
E. coli	Schiff base ligand	22	8	11	14	17
	Ni^{2+} complex	21	14	17	19	22
	Zn^{2+} complex	20	10	13	17	19
	Cd^{2+} complex	21	12	15	18	21
B. subtilis	Schiff base ligand	23	12	14	17	19
	Ni^{2+} complex	24	18	22	25	28
	Zn^{2+} complex	23	13	16	19	21
	Cd^{2+} complex	24	15	18	22	25
S. aureus	Schiff base ligand	19	13	15	17	20
	Ni^{2+} complex	20	19	21	23	25
	Zn^{2+} complex	21	15	17	19	22
	Cd^{2+} complex	21	16	19	21	23
K. pneumonia	Schiff base ligand	18	10	13	17	19
	Ni^{2+} complex	19	17	20	23	25
	Zn^{2+} complex	19	12	15	18	20
	Cd^{2+} complex	18	13	17	20	22

Antifungal activity: The tetradentate Schiff base ligand and its metal(II) complexes were studied for their *in vitro* antifungal activity against *Candida albicans* and *Aspergillus niger* using the agar diffusion method. A solution of Schiff base ligand and metal(II) complexes was spread over agar plates seeded with tested fungi strains in this method. The agar plates were incubated at 35 ºC for 27 h. Clotrimazole, an antibiotic, was used as a standard drug against fungal studies [31]. Both the ligand and its metal(II) complexes were found to good inhibition against all the selected antifungal microorganisms. (Table-6). These findings demonstrated that complexes had significant activity when compared to the Schiff base ligand at different concentrations.

TABLE-6
ZONE OF INHIBITION (mm) OF LIGAND AND ITS METAL(II) COMPLEXES AT VARIOUS CONCENTRATIONS

Strain	Compd.	Control	Concentration (μg/mL)			
			30	60	90	120
C. albicans	Schiff base ligand	22	9	12	14	17
	Ni^{2+} complex	23	16	19	21	24
	Zn^{2+} complex	23	12	15	17	19
	Cd^{2+} complex	23	14	17	19	22
A. niger	Schiff base ligand	20	8	11	13	16
	Ni^{2+} complex	20	16	18	21	25
	Zn^{2+} complex	21	12	14	17	20
	Cd^{2+} complex	20	14	16	18	21

Molecular docking study: An examination using molecular docking was carried out in order to determine the binding contacts of the compounds in question and the orientations of those interactions inside the active region of the target protein. Molecular docking was carried out with MOE on the *E. coli* FabH-CoA complex (PDB ID: 1HNJ) for the purpose of this investigation. FabH is an enzyme that plays a role in the production of fatty acids. It is also the receptor of choice for determining whether or not compounds have the potential to act as antimicrobial agents [32,33]. The crystalline structure of the FabH-CoA complex in *E. coli* was obtained from the protein data bank (http://www.rcsb.org). Docking score (S, Kcal/mol) and hydrogen bond interactions were used to evaluate the binding mechanisms of the compounds with the active site of the target receptor as shown in Fig. 5 and Table-7.

As shown from Table-7, the Schiff base ligand and its metal(II) complexes showed high docking score toward the *E. coli* FabH-CoA complex ranging from -7.53 (CdL) to -7.88 Kcal/mol (NiL) to -8.07 Kcal/mol (ZnL). It was observed that ZnL is the most active one with high docking score (-8.07 Kcal/mol), whereas ZnL showed five hydrogen bond interactions between C22 with THR81, O 11 with ASN193, O27 with

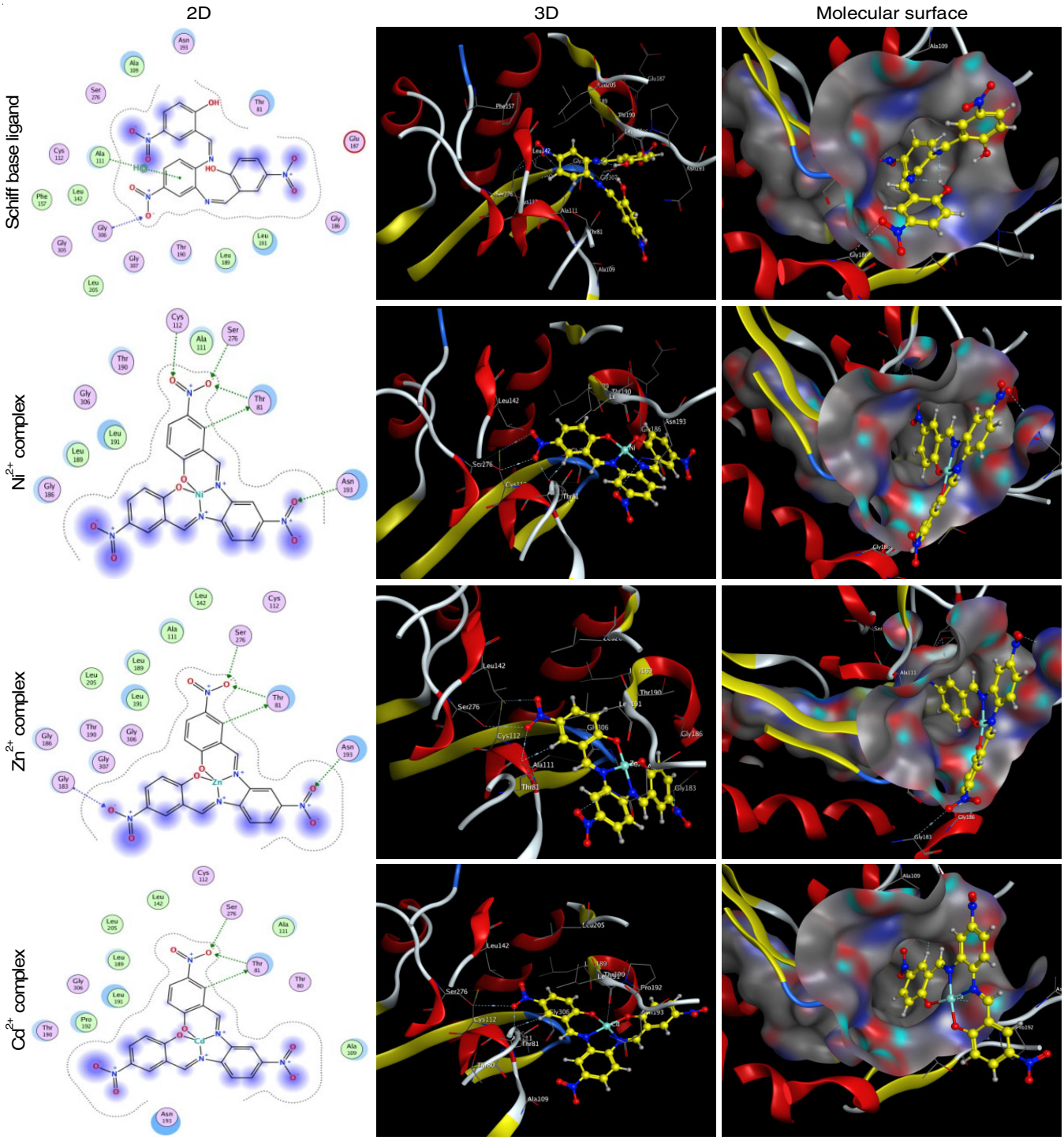

Fig. 5. Molecular docking data

THR81, O27 with SER276 and O30 with GLY183 amino acids residual.

Conclusion

Utilizing 5-nitrosalicylaldehyde and 4-nitro-*o*-phenylenediamine, tetradentate Schiff base ligand and its metal(II), (M = Ni^{2+}, Cd^{2+} and Zn^{2+}) complexes was synthesized and characterized using analytical techniques, including UV-visible, FT-IR, LCMS and conductivity measurements. Antimicrobial activity was tested on the synthesized transition metal (Ni^{2+}, Cd^{2+} and Zn^{2+}) complexes with Schiff base ligand. It was found that the Schiff base ligand and its metal(II) complexes were effective inhibitors of all the studied microorganisms. The metal(II) complexes appear to be non-electrolytes based on the lower molar conductance values. Furthermore, molecular docking was carried out to ascertain the inhibitory action of the studied compounds against *E. coli* FabH-CoA complex (PDB ID: 1HNJ) receptor. Moreover, the molecular structure of the meetal(II) complexes was theoretically optimized and the quantum chemical parameters were calculated and correlated with their biological properties.

TABLE-7
MOLECULAR DOCKING DATA; INTERACTION TYPE AND DISTANCE
BETWEEN LIGAND AND RECEPTOR OF THE SYNTHESIZED COMPOUNDS

	Ligand	Receptor	Interaction	Distance (Å)	E (kcal/mol)	S (kcal/mol)
Schiff base ligand	O10	GLY306	H-acceptor	3.47	-1.10	-6.50
	6-ring	ALA111	pi-H	3.84	-1.30	
Ni^{2+} complex	C22	THR81	H-donor	3.49	-0.80	-7.88
	O11	ASN193	H-acceptor	3.28	-1.10	
	O27	THR81	H-acceptor	3.25	-0.80	
	O27	SER276	H-acceptor	2.99	-1.40	
	O28	CYS112	H-acceptor	3.50	-0.70	
Zn^{2+} complex	C22	THR81	H-donor	3.50	-0.80	-8.07
	O11	ASN193	H-acceptor	3.07	-1.20	
	O27	THR81	H-acceptor	3.27	-0.70	
	O27	SER276	H-acceptor	3.03	-1.40	
	O30	GLY183	H-acceptor	3.34	-1.00	
Cd^{2+} complex	C22	THR81	H-donor	3.51	-0.70	-7.53
	O27	THR81	H-acceptor	3.00	-1.20	
	O27	SER276	H-acceptor	3.32	-0.80	

CONFLICT OF INTEREST

The authors declare that there is no conflict of interests regarding the publication of this article.

REFERENCES

1. C. Boulechfar, H. Ferkous, A. Delimi, A. Djedouani, A. Kahlouche, A. Boublia, A.S. Darwish, T. Lemaoui, R. Verma and Y. Benguerba, *Inorg. Chem. Commun.*, **150**, 110451 (2023); https://doi.org/10.1016/j.inoche.2023.110451
2. N. Dixon and D.R.V. Jones, *Geotext. Geomembr.*, **23**, 205 (2005); https://doi.org/10.1016/j.geotexmem.2004.11.002
3. E. Raczuk, B. Dmochowska, J. Samaszko-Fiertek and J. Madaj, *Molecules*, **27**, 787 (2022); https://doi.org/10.3390/molecules27030787
4. R. Venkatesh, S. Renuka and I. Venda, *Mater. Today Proc.*, **51**, 1810 (2022); https://doi.org/10.1016/j.matpr.2021.10.360
5. K. Deepa and R. Venkatesh, *Int. J. Pharm. Biol. Sci.*, **8**, 29 (2018).
6. A. Mohindru, J.M. Fisher and M. Rabinovitz, *Nature*, **303**, 64 (1983); https://doi.org/10.1038/303064a0.
7. P.R. Palet, B.T. Thaker and S. Zele, *Indian J. Chem.*, **38A**, 563 (1999).
8. M.A. Baseer, V.D. Jadhav, R.M. Phule, Y.V. Archana and Y.B. Vibhute, *Orient. J. Chem.*, **16**, 553 (2000).
9. W. Wang, F.-L. Zeng, X. Wang and M. Tan, *Polyhedron*, **15**, 1699 (1996); https://doi.org/10.1016/0277-5387(95)00403-3
10. O.P. Anderson, A. Cour, M. Findeisen, L. Hennig, O. Simonsen, L.F. Taylor and H. Toftlund, *J. Chem. Soc., Dalton Trans.*, 111 (1997); https://doi.org/10.1039/a603158g
11. A. Tomberg, Gaussian 09w Tutorial. An Introduction to Computational Chemistry using G09W and Avogadro Software, pp. 1-36 (2013).
12. N.A. Elkanzi, H. Hrichi, H. Salah, M. Albqmi, A.M. Ali and A. Abdou, *Polyhedron*, **230**, 116219 (2023); https://doi.org/10.1016/j.poly.2022.116219
13. P. Elmer, ChemBioDraw Ultra Version (13.0.0.3015), CambridgeSoft, Waltham, M.A., USA (2012).
14. Y.A. Alghuwainem, H.M. Abd El-Lateef, M.M. Khalaf, A.A. Abdelhamid, A. Alfarsi, M. Gouda, M. Abdelbaset and A. Abdou, *J. Mol. Liq.*, **369**, 120936 (2023); https://doi.org/10.1016/j.molliq.2022.120936
15. A.D. Becke, *J. Chem. Phys.*, **98**, 5648 (1993); https://doi.org/10.1063/1.464913
16. C. Lee, W. Yang and R.G. Parr, *Phys. Rev. B Condens. Matter*, **37**, 785 (1988); https://doi.org/10.1103/PhysRevB.37.785
17. P.J. Hay, W.R. Wadt, *J. Chem. Phys.*, **82**, 270 (1985); https://doi.org/10.1063/1.448975
18. Y.A. Alghuwainem, H.M.A. El-Lateef, M.M. Khalaf, A.A. Amer, A.A. Abdelhamid, A.A. Alzharani, A. Alfarsi, S. Shaaban, M. Gouda and A. Abdou, *Int. J. Mol. Sci.*, **23**, 15614 (2022); https://doi.org/10.3390/ijms232415614
19. H. Hrichi, N.A. Elkanzi, A.M. Ali and A. Abdou, *Res. Chem. Intermed.*, **49**, 2257 (2023); https://doi.org/10.1007/s11164-022-04905-4
20. A. Abdou, O.A. Omran, A. Nafady and I.S. Antipin, *Arab. J. Chem.*, **15**, 103656 (2022); https://doi.org/10.1016/j.arabjc.2021.103656
21. A. Abdou and A.-M.M. Abdel-Mawgoud, *Appl. Organomet. Chem.*, **36**, e6600 (2022); https://doi.org/10.1002/aoc.6600
22. N.A.A. Elkanzi, A.M. Ali, H. Hrichi and A. Abdou, *Appl. Organomet. Chem.*, **36**, e6665 (2022); https://doi.org/10.1002/aoc.6665
23. M.A. Arafath, F. Adam, M.B.K. Ahamed, M.R. Karim, M.N. Uddin, B.M. Yamin and A. Abdou, *J. Mol. Struct.*, **1278**, 134887 (2023); https://doi.org/10.1016/j.molstruc.2022.134887
24. A. Abdou, H.M. Mostafa and A.-M.M. Abdel-Mawgoud, *Inorg. Chim. Acta*, **539**, 121043 (2022); https://doi.org/10.1016/j.ica.2022.121043
25. A.M. Abu-Dief, N.H. Alotaibi, E. S.Al-Farraj, H.A. Qasem, S. Alzahrani, M.K. Mahfouz and A. Abdou, *J. Mol. Liq.*, **365**, 119961 (2022); https://doi.org/10.1016/j.molliq.2022.119961
26. A. Kumar, D. Kumar, K. Kumari, Z. Mkhize, L.M.K. Seru, I. Bahadur and P. Singh, *J. Mol. Liq.*, **322**, 114872 (2021); https://doi.org/10.1016/j.molliq.2020.114872
27. E.K. Shokr, M.S. Kamel, H. Abdel-Ghany, M.A.E.A.A.A. El- Remaily and A. Abdou, *Mater. Chem. Phys.*, **290**, 126646 (2022); https://doi.org/10.1016/j.matchemphys.2022.126646
28. W.J. Geary, *Coord. Chem. Rev.*, **7**, 81 (1971); https://doi.org/10.1016/S0010-8545(00)80009-0
29. M. Govindarajan, M. Karabacak, V. Udayakumar and S. Periandy, *Spectrochim. Acta A Mol. Biomol. Spectrosc.*, **88**, 37 (2012); https://doi.org/10.1016/j.saa.2011.11.052
30. P. Politzer and D.G. Truhlar, eds., Chemical Applications of Atomic and Molecular Electrostatic Potentials: Reactivity, Structure, Scattering and Energies of Organic, Inorganic and Biological Systems, Plenum: New York (1981).
31. B. Ehresmann, B. Martin, A.H.C. Horn and T. Clark, *J. Mol. Model.*, **9**, 342 (2003); https://doi.org/10.1007/s00894-003-0153-x
32. V.S. Mironov, T.A. Bazhenova, Yu.V. Manakin, K.A. Lyssenko, A.D. Talantsev and E.B. Yagubskii, *Dalton Trans.*, **46**, 14083 (2017); https://doi.org/10.1039/C7DT02912H
33. N.A.A. Elkanzi, A.M. Ali, M. Albqmi and A. Abdou, *Appl. Organomet. Chem.*, **36**, e6868 (2022); https://doi.org/10.1002/aoc.6868